ORIGINAL ARTICLE

Exploring the microstructure of hydrated collagen hydrogels under scanning electron microscopy

Daniel J. Merryweather[1] | **Nicola Weston**[2] | **Jordan Roe**[1,3] |
Christopher Parmenter[2] | **Mark P. Lewis**[4] | **Paul Roach**[1]

[1]Department of Chemistry, School of Science, Loughborough University, Leicestershire, UK

[2]Nanoscale and Microscale Research Centre, University of Nottingham, Nottingham, UK

[3]Department of Materials, Loughborough University, Leicestershire, UK

[4]National Centre for Sport and Exercise Medicine (NCSEM), School of Sport, Exercise and Health Sciences, Loughborough University, Leicestershire, UK

Correspondence
Dr. Paul Roach, Department of Chemistry, School of Science, Loughborough University, Leicestershire, UK.
Email: p.roach@lboro.ac.uk

Abstract

Collagen hydrogels are a rapidly expanding platform in bioengineering and soft materials engineering for novel applications focused on medical therapeutics, medical devices and biosensors. Observations linking microstructure to material properties and function enables rational design strategies to control this space. Visualisation of the microscale organisation of these soft hydrated materials presents unique technical challenges due to the relationship between hydration and the molecular organisation of a collagen gel. Scanning electron microscopy is a robust tool widely employed to visualise and explore materials on the microscale. However, investigation of collagen gel microstructure is difficult without imparting structural changes during preparation and/or observation. Electrons are poorly propagated within liquid-phase materials, limiting the ability of electron microscopy to interrogate hydrated gels. Sample preparation techniques to remove water induce artefactual changes in material microstructure particularly in complex materials such as collagen, highlighting a critical need to develop robust material handling protocols for the imaging of collagen hydrogels. Here a collagen hydrogel is fabricated, and the gel state explored under high-vacuum (10^{-6} Pa) and low-vacuum (80–120 Pa) conditions, and in an environmental SEM chamber. Visualisation of collagen fibres is found to be dependent on the degree of sample hydration, with higher imaging chamber pressures and humidity resulting in decreased feature fidelity. Reduction of imaging chamber pressure is used to induce evaporation of gel water content, revealing collagen fibres of significantly larger diameter than observed in samples dehydrated prior to imaging. Rapid freezing and cryogenic handling of

the gel material is found to retain a porous 3D structure following sublimation of the gel water content. Comparative analysis of collagen hydrogel materials demonstrates the care needed when preparing hydrogel samples for electron microscopy.

KEYWORDS
drying artefact, hydration, hydrogel, imaging, microstructure, scanning electron microscopy

1 | INTRODUCTION

Hydrogels are soft materials comprised a 3D network of hydrophilic polymers suspended in water which may swell or shrink as the degree of hydration varies. Hydrogels are capable of absorbing and retaining a large quantity of water relative to the polymer mass, by the association of water molecules around the polymer chains, which are stabilised by reversible hydrogen bonds and molecular cross-linking. The degree of hydration and dynamic exchange of liquid and solute content between gel and environment is highly desirable in the field of tissue engineering[1] and manufacture of controlled drug-delivery devices.[2] In the advent of new technologies such as bioprinting rapidly expanding,[3] there is an increasing need to develop robust methods to assess the microscale structure and determine the relationship between observed material structure and functional properties in use. Scanning electron microscopy is a powerful tool to interrogate material microstructures; however, preparation and handling of soft hydrated biological samples has been identified as a serious technical challenge.[4]

Collagen is the most abundant ECM peptide found in the animal kingdom. There are 28 types of human collagen identified within the collagen superfamily, each with numerous isoforms and possible post-translation modifications.[5] Six α-chain molecules have been identified and collagen types differentiated by constituent α chains.[5] The tight packing of the collagen triple helix necessitates glycine at every third residue, resulting in the frequent triplet motif Gly X Y, where X is typically a proline residue, and Y either hydroxyproline, lysine, or hydroxylysine. The triple helical collagen molecule is 1.5 nm in diameter and 300 nm in length. Individual collagen molecules are assembled by a network of water-mediated hydrogen bonds into fibres and fibre aggregates[6] which may range in diameter in humans from ~500 nm in the vitreous of the eye[7] and up to 400 μm in the tendon fascicle.[8] The organisation of collagen fibres in biological tissues imparts mechanical properties such as tensile strength and elasticity that in turn enable function[9] and guide cell behaviour.[10] The staggered arrangement of collagen molecules into

fibres produces a distinct 'D-band' at points of highest collagen density with a periodicity of 67 nm. This banding is apparent in both native and reconstituted collagens, allowing for ready identification under electron microscopy (Figure 1), presenting as a darker region due to the higher density of collagen molecules at these points.[11]

Water plays a key role in the macrostructure of collagen fibres through its interaction with hydroxyamino acids of the collagen molecule. The presence of water enables bridging of hydrogen bonding between collagen molecules within a collagen fibre at longer distances than under dehydrated conditions. Under hydrated conditions, the interfibrillar space of a collagen fibre increases due to this bridging effect of water on the hydrogen bonding between hydroxyamino acids.[12] This is reflected both at a macro- and molecular scale.[13] Dehydration of collagenous biological tissues such as bone[14,15] and tendon[13] has been observed to significantly alter the biomechanics of these tissues which is thought to stem from this change in the physical structure of the collagen matrix.

The expansion and contraction of interfibrillar space with relation to water content has been modelled
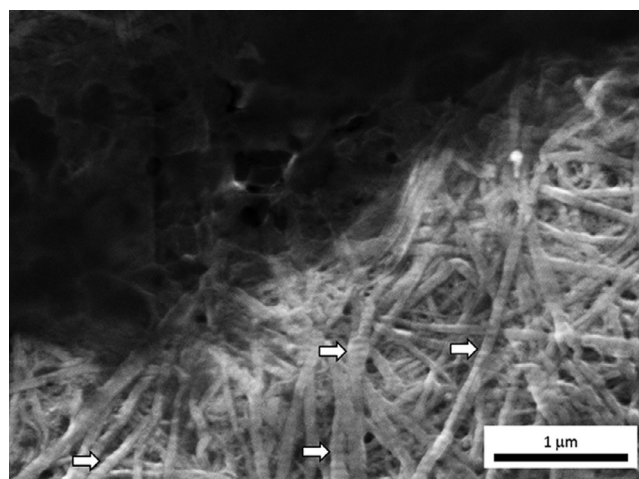
FIGURE 1 The presentation of D-banding of collagen fibres under FEG-SEM. A pattern of banded dark regions (examples indicated by white arrows) is observed. This phenomenon is created by the increased density of collagen fibrils at these points.

extensively in silico[16–18] and observed in vitro under AFM probing of collagen fibres under varying degrees of local humidity or hydration.[19–21] The interaction between the collagen triple helix and water, therefore, plays a critical role in the structural organisation of collagen, and its removal generates conformational changes, leading to molecular contraction and the induction of significant tensile stresses up to the MPa range.[12]

As a ubiquitous feature of mammalian tissue matrices, collagen is an appealing platform for biopolymer tissue engineering.[22] Collagenous materials are readily broken down by acid treatment, producing a solubilised collagen widely employed in tissue engineering.[23] Collagen fibres are reconstituted into a gel state by neutralisation of the acid solution, which allows hydrogen bonds between collagen molecules to reform, and by treatment with cross-linking enzymes such as lysyl oxidase,[24] forming a random network of collagen fibres.

Collagen microstructure and organisation has been explored extensively using atomic force microscopy.[19,25,26] While this approach requires minimal sample preparation, imaging large areas greater than a few microns is time consuming and ability to observe the internal structure of gel materials is limited due to limited penetration of the probe into the material on the *z*-axis. Collagen fibre orientation can be assessed using polarised Fourier-transform infrared spectroscopic imaging[27]; however, here maximum resolution is well above the size of many collagen fibres.

SEM is a gold standard technique to directly visualise the micro- and nanoscale structure of materials. An electron stream is directed onto the sample surface. Upon impact with the sample, x-rays are emitted dependent upon the atomic composition of the sample, as well as secondary electrons released from their orbitals. Bombardment of a sample with sufficiently high-energy electrons for prolonged periods may result in ablation of the sample surface which may be deleterious in the study of soft materials. A portion of emitted electrons experience a change in direction and may be detected as a backscattered electrons with an energy above 50 eV. Backscattered electrons typically have poor resolving power; however, their high energy allows for penetration through, and escape from, relatively thick materials. The backscattering of electrons is influenced by atomic number and relative density along the electron beam, hence detection of backscattered electrons allows for the determination of density variations within a sample, such as identification of metal grain size and crystal orientation.[28] Secondary electrons emitted from the sample typically have an energy range up to 50 eV. The low energy of these electrons limits the distance from the primary electron from which they are generated, and the depth of the sample through which they can escape to be detected, limiting their use to surface imaging. Material edges and similar regions present high surface areas from which secondary electrons can escape, hence these regions appear brighter in secondary electron imaging and so readily provide a depth of field and sense of topography to the generated image.

As scanning electron images are generated by the backscattering of electrons and release of secondary electrons, image generation is sensitive to the charging of particles within the imaging chamber. Charging results in the presence of ions, which may capture released electrons or cause deflection of their flight path away from electron detectors. Liquid water in particular presents a serious issue due to its high ionisation potential, radical generation and near ubiquitous presence in the environment.[29] The presence of gaseous molecules in the imaging chamber creates the potential for in-flight interaction between emitted electrons and this gaseous environment, resulting in artefactual detection. These concerns limit the use of SEM in the analysis of biological samples under physiological conditions; samples are generally dehydrated and held under vacuum to ensure minimal charging, conditions inimical to proper biological function and the stability of many biological structures. This in turn renders the imaging of hydrated materials such as hydrogels a serious technical challenge under standard SEM protocols.

As the structure of hydrogels is so closely linked to the degree of hydration (Figure 2), dehydrated films imaged under SEM do not necessarily reflect the structure of the hydrated gel. Artefacts are induced by, for example, shrinkage and loss of 'pores' or void spaces of the gel as the polymer material is made increasingly concentrated by the creeping loss of the gel's water content.[30] This loss of water content, as the bulk volume of the gel, results in a densification of the gel polymer, reducing apparent porosity and potentially generating polymer aggregates that are not present in the hydrated material, and generally disrupting the polymer network relative to how these features exist in the hydrated gel state.

Cryogenic handling of hydrated materials (below −140°C) allows for preservation of fine-detail structures by vitrification of the gel water content and minimisation of expansion during freezing.[31] Bringing a gel material to below the freezing point of water because the process of ice crystal nucleation. As the sample freezes, the expansion of these ice crystals causes distortion of the gel polymer network. Ice crystal size can be minimised by increasing the rate of cooling through the sample to ensure a rapid phase transition of gel water content from liquid to solid while limiting the growth of nucleated ice crystals.[32,33] Complete vitrification of a gel's water content can be induced by extremely rapid freezing of samples with small volumes, as the small dimensions involved ensure rapid equilibration of temperature throughout the
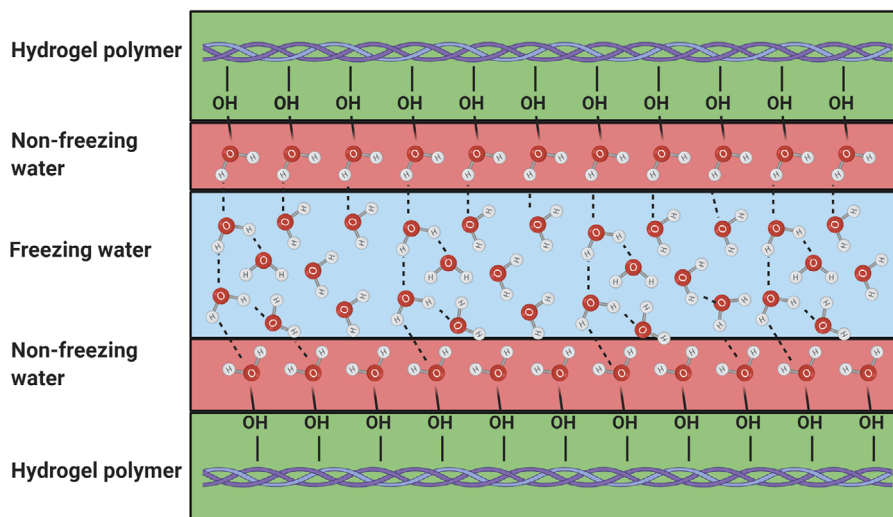
FIGURE 2 The hydration shell in hydrogel materials. Hydrogel stability is maintained by extensive hydrogen bonding with water molecules, forming a hydration shell around the hydrogel polymer network. Water molecules in close association with the hydrophilic polymer network of the hydrogel become tightly bound and play a role in maintaining the structure of the gel polymer network. High energy required to dissociate this close association results in 'nonfreezing' water layers distinct from the bulk freezing water layer that maintains minimal contact with the polymer network. As hydrogels are dehydrated, water is first lost from bulk freezing layers resulting in contraction of the gel material. In a collagen fibrillar network, this results in a decrease in the interfibrillar space.

material being prepared. This can be achieved by plunging a sample into a cryogen provided sample thickness does not exceed ~20 μm[32] or by use of high-pressure freezing in thicker samples.

In this manner, the microstructure of gel polymers can be preserved without damage induced by water ice crystallisation during freezing. Cryogenic handling of materials also reduces the inherent kinetic energy of constituent particles and so limits the degree of molecular stress within the sample. The relationship between gel hydration, freezing rate, elastic strength, and the generation of imaging artefacts has recently been explored in depth using glycerol methacrylate and hydroxyethyl methacrylate hydrogels demonstrating the relationship between the elastic moduli of gel polymers in hydrated states, and the impact of water ice crystallisation in distorting the polymer network.[33]

With control of sample chamber environment, evaporation of gel water content can be induced under cryogenic conditions while allowing for preservation of the 3D organisation of gel polymer as exists in the hydrated gel state.[34] Handling of sample water content during preparation is a notable source of artefact inducement in biological materials, generally necessitating rapid freezing to preserve ultrastructure.[35,36] Rapid freezing can have deleterious effects on biological materials resulting in a trade-off between preservation of larger-scale anatomical ultrastructure against preservation of cellular and molecular scale features of interest.[37]

Environmental SEM (ESEM) allows for the maintenance of relatively high pressures within the imaging chamber of electron microscopes while retaining as near to vacuum conditions as possible around the electron beam emission source.[38] A series of apertures and vacuum pumps are used to create segregated regions of pressure along the electron beam path, such that the electron beam passes through only a short distance of relatively high pressure before engaging with the sample. This allows for an environment to be maintained at pressures nearing 100 mbar within the sample imaging chamber while the electron emission source remains under high-vacuum conditions. In the ESEM chamber, emitted electrons interact with the sample as in standard SEM to produce secondary electrons. These then interact with the gaseous molecules of the loaded environment to generate a cascade of gaseous secondary electrons and charged particles. The electron cascade is utilised by a series of gaseous secondary electron detectors (GSEDs) to generate the sample image, while charged particles of the gas interact with the sample surface to negate surface charging generated by the production of secondary electrons. Due to these conditions, sample imaging under ESEM can be carried out at similar levels of magnification to standard SEM without the need for processing and coating of hydrated materials. Dynamic reactions and changes in the distribution of water can be observed on the microscale and in real-time. Conditions within the sample chamber can be controlled to adjust the temperature and pressure the sample is

imaged under. Such manipulation can induce, for example, in situ freeze-drying in which water within a sample is rapidly frozen and evaporated by low-temperature and low-pressure conditions.[39]

In this study, fabricated type I collagen hydrogels were interrogated under SEM with varying methods and compared to observe structural changes induced in the samples. Collagen films were prepared by dehydration of collagen hydrogels under standard conditions and assessed by field-emission gun (FEG) SEM under vacuum. This is contrasted with the hydrated collagen gel state prepared by plunge-freezing to determine the role of hydration in maintaining fibre orientation and gel porosity. Finally, collagen hydrogels were explored under environmental and low-pressure imaging conditions under water vapour or nitrogen atmosphere, to assess the ability of these imaging modes to visualise microscale features of the hydrated gel state without the need for cryogenic handling or heavy metal coating.

2 | METHODS AND MATERIALS

2.1 | Collagen hydrogel fabrication

Collagen hydrogels were fabricated by neutralisation of acid-soluble rat-tail type I collagen. Solubilised collagen at 2.05 mg/mL suspended in 0.6% v/v acetic acid and 10× MEM was purchased from First Link UK. Solubilised collagen solution (850 μL) was mixed with 130 μL of 10× MEM (First Link UK) to provide an indication of solution pH. Sodium hydroxide (2 M, ~20 μL) was added to neutralise the solution and induce fibrillogenesis. Collagen gels were cast into 24-well plates with 500 μL per well and incubated at 37°C for 15 min to allow for complete gelation. Collagen gels were either kept hydrated until imaging or dehydrated as described.

2.2 | High-vacuum SEM

Deposited collagen films were dehydrated by standing at room temperature at one atmosphere pressure for a 2-week period. Dried samples were sputter-coating with an 80:20 Au/Pd using a Quorum Technologies Q 150 TES coater (Quorum Technologies, Loughton, UK), for 90 s at 20 mA to give a coating ~8 nm thick. Samples were attached to aluminium sample stubs (TAAB Laboratories) using double-sided carbon tape and imaged on a JEOL 7800F FEG-SEM at 2 or 5 kV with a working distance of 10 mm. Image acquisition was carried out at ×1000 and ×10,000 magnification.

2.3 | Cryogenic SEM and FIB milling

Hydrated gel samples were imaged using an FEI Quanta 200 3D (FEI, Hillsboro, Oregon, USA) focused ion beam (FIB) SEM to explore the internal architecture of a hydrated gel in its native state. To enable cryo-SEM, the system was equipped with a Quorum 3010 cryostage and preparation chamber (Quorum Technologies, Loughton, UK). Collagen gel samples of 2 μL were excised using a positive displacement pipette and transferred onto a magnetic O-ring holder. This O-ring was attached to a Leica-Reichert EM MM80 E metal-mirror-freezer for cryofixation. The sample stub was rapidly dropped onto a gold-coated high-purity copper block cooled in liquid nitrogen to induce rapid freezing through the sample while damping weight during impact to minimise compression of the sample material. The frozen sample was transferred to the mobile TEM-Prep Slusher and mounted to the cryoshuttle in slushy nitrogen. Using the airlock transfer adapter, the sample was removed from liquid nitrogen immersion and transferred to the sample preparation airlock precooled to −175°C. Within the preparation airlock, gel samples were sputter-coated with Pt for 60 s at 10 mA producing a coating ~2.5 nm. The sample was transferred to a −175°C precooled imaging chamber. Further platinum was layered upon the sample surface by gas injection of methylcyclopentadienyl platinum precursor gas (pt-GIS of the Quanta 3D), generating a surface coating of platinum. A series of 30 μm by 15 μm trenches were milled into the gel surface by application of a 3 nA focused Ar+ ion beam, further smoothing the revealed ice face using a 0.3 nA focused Ar+ ion beam. Samples were moved to the airlock under vacuum and temperature was raised from −175°C to −90°C for 30 min to induce sublimation of the gel water content at the cut surface. Smoothing of the gel ice face in milled trenches ensured that sublimation of water from this exposed face occurred evenly across the surface. Samples were cooled to −175°C and returned to the imaging chamber.

2.4 | Environmental SEM

Collagen samples were directly imaged using an FEI Quanta 650 ESEM (FEI, Hillsboro, Oregon, USA) with a thermionic tungsten filament source. This source of electrons is known to produce images of a lower quality than FEG sources such as a tungsten tip due to the much larger surface area from which electrons are emitted. Samples were loaded onto a precooled stub at 4°C. ESEM images were captured using a GSED, using 10 kV under an atmosphere of water vapour at 1000 Pa. After initial imaging of the hydrated gel sample, imaging chamber temperature
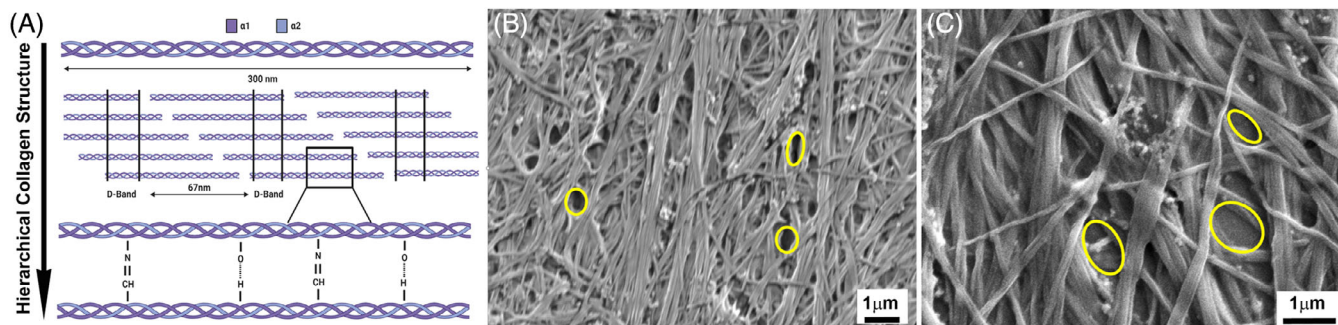
FIGURE 3 Hierarchical structure of collagen. (A) Composed of a repeating primary sequence, collagen molecules are organised into a triple helix, in turn present in a staggered arrangement to form fibres. Fibre bundles are maintained by a dynamic hydrogen bonding network and enzymatic crosslinks. (B, C) Representative images of dehydrated collagen films under vacuum FEG-SEM. Pores highlighted by yellow circles are presented as gaps between collagen fibres.

was dropped from 4 to −20°C and pressure dropped from 1000 to 100 Pa while maintaining consistent humidity to induce in situ freeze-drying of the gel sample.

2.5 | Low-vacuum SEM

Bulk gel samples were imaged using the FEI Quanta 650 ESEM (FEI, Hillsboro, Oregon, USA) in low-vacuum mode (80–120 Pa) using the large field detector (LFD). Imaging was conducted under water vapour or nitrogen atmospheres to assess the impact of gel-gas interaction at the surface. Gel samples were placed onto a precooled sample stub held at −15°C prior to loading into the electron microscope to freeze the gel water content. Atmospheric pressure within the sample chamber was lowered during imaging from 200 to 50 Pa to induce in situ evaporation. Imaging chamber humidity under water vapour atmosphere was decreased with decreasing pressure and so was not maintained at a consistent level throughout imaging.

2.6 | Image analysis and statistics

All images were analysed using the Fiji ImageJ image processing package.[40] Statistical analysis was conducted using Origin 2019, using ANOVA to compare variance of means with post hoc Tukey's test to assess significance of variance between data groups.

3 | RESULTS

3.1 | Air-dried gel films

Collagen films prepared by dehydration of collagen hydrogels at room temperature were imaged under vacuum by FEG-SEM. Dehydration and a gold/palladium coating
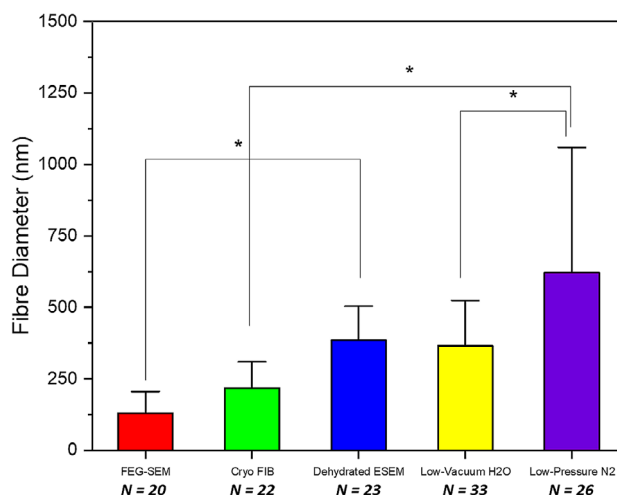
FIGURE 4 Comparison of average fibre diameters under SEM imaging conditions. Imaging of dehydrated films conditions and of cryogenically handled hydrated gels under vacuum conditions produced no significant difference in fibre diameter. Similarly imaging of dehydrated films under environmental pressure and hydrated gels under low-vacuum water vapour atmosphere did not produce significantly different fibre diameters. Fibre diameters under nitrogen low-vacuum atmosphere were significantly larger; however, this was the result of a large aggregation of fibres within a complex 3D network not visible under water vapour imaging.

were employed as a baseline measure of 'standard' collagen sample preparation for electron microscopy. Chemical fixatives such as formaldehyde or glutaraldehyde were not used to minimise the introduction of artefacts within the collagen fibre network created by chemical crosslinking. Collagen fibres were readily identified as a series of smaller-diameter fibrils closely associated to form larger observable fibres (Figure 3). Fibres extended across field of view being 10s of micrometres in length. Smaller-diameter fibrils were frequently observed to interact with larger aggregates, braiding into larger fibres at points along their length. Average fibre diameter (Figure 4) was found to
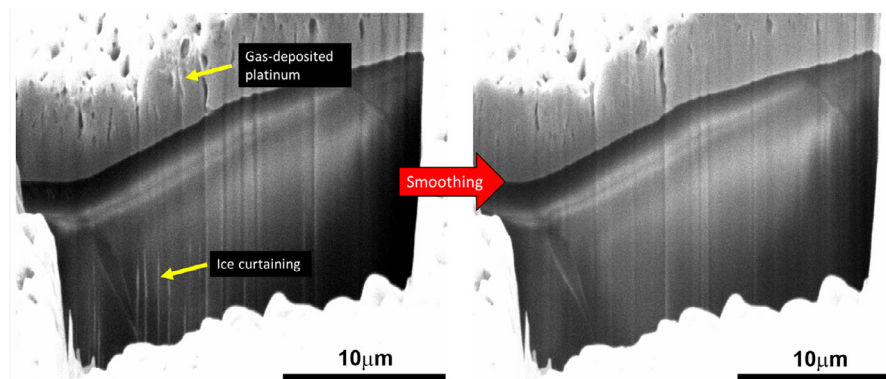
FIGURE 5 Preparation of cryogenic hydrated collagen gels for SEM imaging. Platinum is deposited onto the sample surface by gas injection. A focused ion beam is applied to excavate an exploratory trench. The surface of the revealed ice face is smoothed by further low-intensity milling to reduce ice curtaining generated by differences in the thickness of the deposited platinum layer across the gel surface.

be 130.5 ± 75.4 nm. While interfibre gaps were readily identified, 'pore' size varied dramatically according to the local orientation and placement of collagen fibres, with 'pores' of 100 ± 90 nm^2 formed from the area within a region surrounded by intersecting collagen fibres rather than a cohesive molecular structure. A comparison of feature sizes as measured is presented in Figure 4, although some are not well resolved.

3.2 | Cryo-SEM prepared gels

Imaging of plunge-frozen collagen hydrogels handled under cryogenic conditions demonstrated good preservation of collagen fibre distribution within the hydrated gel state. This technique produces vitreously frozen material particularly at the sample surface where imaging was carried out, with minimal ice crystal artefacts, compared to gels frozen in slushy nitrogen. This allows for confident imaging of the porous structure of the gel in its hydrated state with relatively minimal disruption induced by the crystallisation of water ice during freezing. Gas-phase deposition of platinum prior to milling was used in order to protect the bulk gel surface. This layer is highly granular leaving regions with a variable degree of protection to the ablating ion beam. Once applied this variability induces ablation of the ice face at a variable rate, sometimes resulting in difficulties producing a completely smooth surface prior to sublimation, known as curtaining. Exploratory trenches were smoothed by low current focused ion-beam milling (0.3–0.5 nA) in order to reduce curtaining of the retreating ice face during sublimation. However, a degree of curtaining was found to be present in most trenches (Figure 5).

Following sublimation of gel water content in cryogenically handled collagen samples by raising sample temperature to −90°C, imaging of excavated trenches revealed a well-dispersed network of fibres throughout the imaging space (Figure 6). Average fibre diameter was found to be in agreement with measurements of dehydrated collagen film samples at 217.5 ±92 nm, indicating minimal aggregation of fibres during the drying processes. However, average pore size was found to be significantly larger in freeze dried samples, at 1200 ± 75 nm^2, compared to samples dehydrated at room temperature and one atmosphere pressure (Figure 6D). This suggests that the fully dehydrated collagen film observed in Figure 3 represents a densified gel state in which water-filled 'pores' or voids have shrunk as the gel water content was lost.

3.3 | ESEM in situ dehydration

Collagen films dehydrated under standard conditions were imaged under environmental scanning electron microscopy via GSEDs, under a water vapour atmosphere. While individual collagen fibres were readily distinguished (Figure 7), finer details of the collagen fibres were difficult to resolve even at higher magnification. Braiding and aggregation of individual smaller-diameter fibres could not be resolved, resulting in a larger average fibre diameter relative to secondary electron imaging under a vacuum environment at 385 ±119 nm (Figure 4).

Hydrated collagen hydrogels were imaged under a 1000 Pa water vapour atmosphere using GSEDs. Surface features could not be readily identified, with the gel surface presenting as a largely flat plane absent of the fibrillar structures observed under vacuum SEM (Figure 8). Imaging of the gel surface was observed to rapidly induce ablation of the gel water content. In situ evaporation of gel water content revealed a striated pattern on the gel surface as the water was removed (Figure 8C). Distinct features of collagen fibres, however, remained largely unresolved, with large gel artefacts initially being
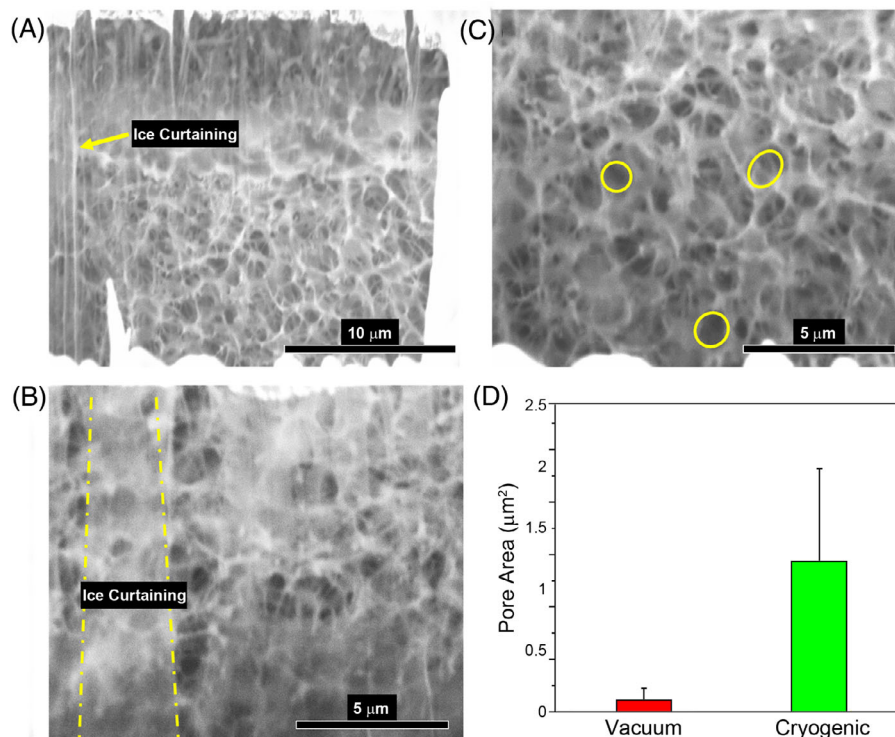
FIGURE 6 Sublimation of cryogenically handled hydrated collagen gels revealed a 3D network of fibres with large area pores. (A, B) Ice curtaining was visible in many milled trenches due to the irregular gas-deposited platinum coating. (C, D) Pores (yellow circles) were found to be of significantly larger dimensions in hydrated gels compared to those ambiently dehydrated and observed under vacuum.

determined (Figure 8A and B), followed by apparent stratified features at lower pressures.

3.4 | Low-vacuum SEM

Hydrated collagen gels were imaged under low-vacuum conditions using the large field detector (Figure 9). Gels were rapidly frozen in situ immediately prior to depressurising of the imaging chamber atmosphere. At pressures above 100 Pa, the frozen gel presented as a smooth surface with no readily identifiable features. Below 100 Pa, fibrous structures became increasingly apparent as the gel water content evaporated, but with some ice formation imparting roughness on the surface (Figure 9C). Frozen collagen gels were imaged under both water vapour and nitrogen atmospheres. Identification of fibrous structures under water vapour atmosphere was noticeably more difficult, with reduced contrast between collagen fibres and the gel ice surface. In contrast, evaporation under nitrogen atmosphere revealed large regions filled with readily identifiable fibrous structures (Figure 9D–F). Although branching of these structures was apparent, individual fibre diameters could not be reliably measured, resulting in large apparent fibre diameters under nitrogen low-pressure atmosphere relative to water vapour low-pressure

atmosphere. Average fibre diameters under water vapour imaging were found to be 364 ± 159 nm compared to 623 ± 437 nm under nitrogen imaging.
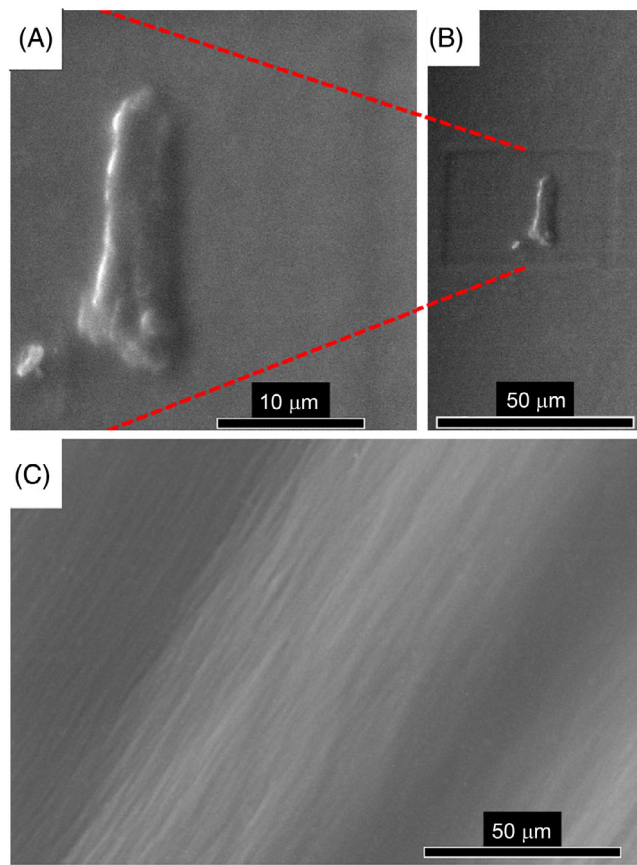
4 | DISCUSSION

Hydrogel structure is intrinsically linked to the presence of a hydration shell around the gel polymer, in this case collagen molecules arranged into a network of fibres, and overall degree of hydration,[30] forming distinct layers of bound water according to the degree of energy associated with the binding.[41] Water molecules in closer association to the hydrophilic polymer network of the hydrogel interact more strongly with this network, and so require more energy to become dissociated. This results in nonuniform states of water within the gel material, with tightly bound 'nonfreezing' water in close association with the polymer network, a series of transitional layers of bound freezing water that dynamically interact with the polymer network but are not tightly bound and can be frozen, and free water that moves freely through the gel without associating with the hydrophilic polymer network. Due to this close association between hydrophilic gel polymer network and gel water content, loss of gel water content occurs in a series of step transitions according to the energy requirements
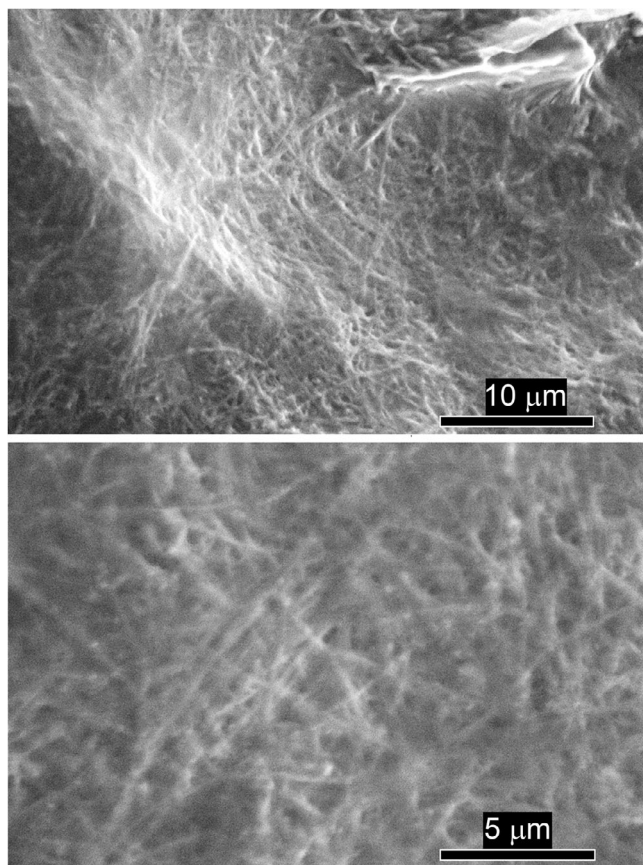
FIGURE 7 ESEM imaging of dehydrated collagen films. Collagen fibres were readily identified; however, identification of constituent fibrils was obscured. Under gaseous secondary ion detection pore spaces between fibres could not be determined.

FIGURE 8 ESEM imaging of hydrated collagen hydrogel. (A, B) Surface features were poorly resolved and could not be identified at environmental pressure. (C) As pressure was reduced to 100 Pa striated features appeared on the gel surface. Firm confirmation of these features as the underlying collagen fibre network was not achieved due to the limits of resolving higher magnification images under this mode.

to dissociate these two components of the gel material. Free water is rapidly lost from the gel material, followed by bound freezing water, and finally by the closely associated nonfreezing hydration shell.

In this work, the role of this hydrogel hydration shell can be readily observed in terms of its influence on imaging resolution and microscale feature fidelity when attempting to image the polymer network of the gel. Dehydration of the collagen gel to form a collagen film produced readily identifiable collagen fibres (Figure 3) in which the lack of hydration allows for full penetration of secondary electrons through intermolecular spaces within the fibre, and so resolution of nanoscale detail such as the aggregation and braiding of small fibrils into larger fibre units. Under cryogenic handling of the collagen gel material, rapid freezing and maintenance of a low-energy environment preserves the interfibrillar spacing of 3D collagen fibre network. Fibre diameter in this hydrated state is found to be in good agreement with observations of dehydrated collagen films, indicating imaged 3D networks within the hydrated gel state represent individual collagen fibres or small aggregates. Pore size is found to decrease an order

of magnitude following dehydration at room temperature and one atmosphere pressure, with the loss of the gel water content resulting in densification of the collagen fibre network and reduction of void spaces previously filled with water. Preparative methodologies for hydrated samples are known to distort native gel morphologies and impact molecular interactions on the nanoscale.[42–44]

Under ESEM, imaging of dehydrated collagen films was found to produce significantly larger observed average collagen fibre diameters (Figure 4). As films were imaged under a water vapour atmosphere, it is likely that imaging fidelity was reduced by the interaction of free water molecules within the environment with hydrophilic collagen fibres. As this hydration shell of bound water is restored, the penetration of secondary electrons through the fibre is likely inhibited. Imaging of hydrated collagen gels under ESEM similarly demonstrated the impermeability of water to secondary electrons (Figure 8). Although striated features were observed following in situ
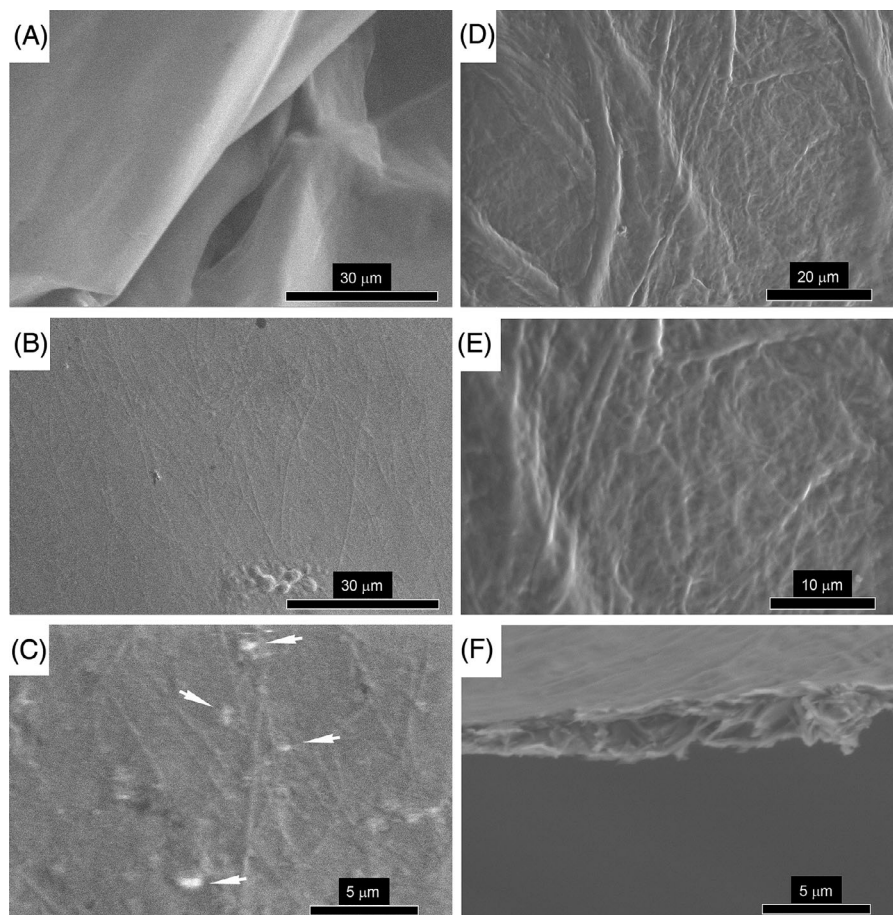
FIGURE 9 Low-vacuum imaging of hydrated collagen hydrogel. (A–C) Imaging under a water vapour atmosphere. As pressure decreased, individual fibres emerged from the ice surface. (D–F) Imaging under a nitrogen atmosphere. As pressure was decreased, a widespread network of fibres partially obscured by a residual hydration shell could be visualised. As evaporation continued, the 3D organisation of individual fibres was well resolved (F). White arrowheads in (C) indicate ice crystal formation.

evaporation of the gel water content, these were difficult to measure individually and could not be resolved to identify individual fibres even at comparatively low magnifications. Imaging of uncoated samples under ESEM was found to induce significant damage to the sample surface, even at low accelerating voltages (data not shown) further making this a less desirable approach.

Hydrated collagen hydrogels initially presented under low-pressure atmospheres as a solid surface of water ice with few distinguishable features. As pressure was decreased below 100 Pa, evaporation of this water ice was induced, and collagen fibres were gradually revealed. Visualisation of the collagen fibre network was found to be limited under a water vapour atmosphere with few fibres emerging from the water ice surface over time. In contrast, under a nitrogen atmosphere, a widespread 3D network of collagen fibres could be observed. Under a water vapour atmosphere, imaging chamber humidity can be controlled by control of water vapour pressure and chamber temperature to maintain a saturated vapour pressure.[45] This is essential to minimise uncontrolled evaporation of sample water to the environment, and condensation of environmental water onto the sample as ice. In this study chamber, humidity was poorly controlled, perhaps due to the high water content of the gel samples being imaged. As the collagen molecule itself strongly associates with water, it is likely that poor control of water within the imaging chamber allowed for interactions between environmental water, sample water and exposed collagen molecules. Ice deposition was frequently observed over exposed collagen fibres, as demonstrated in Figure 9C, indicating that environmental water was condensing onto the gel sample. In contrast, environmental pressure could be lowered under a nitrogen atmosphere to induce evaporation of gel water content. Free unbound water is then lost from the gel volume resulting in the exposure of collagen fibres and a visible hydration shell that occludes resolution of fine detail. At points of fracturing with a high exposed surface area, increasingly fine detail was resolved as this hydration shell was reduced in volume more rapidly (Figure 9F).

5 | CONCLUSIONS

Handling and preparation of soft hydrated materials for imaging under electron microscopy can introduce system-wide changes in micro- and nanoscale presentation of the material. A dramatic rise in the use of collagen hydrogels, and our understanding of how such fine features can impart huge variation in material properties, has highlighted a need to better understand the presentation of collagen gels in their hydrated state. With a wealth of developing imaging modalities, we demonstrate here the imparted structural changes on a collagen hydrogel during sample preparation and imaging, including fibre diameter and pore size. As these changes are induced by the preparation route for each imaging mode, the effect of sample preparation needs to be understood by those choosing a method of observation prior to beginning experiments.

The dehydration of collagen hydrogels at room temperature under one atmosphere, without the use of chemical fixatives, is found to be a robust method to visualise collagen fibres. While the resulting dehydrated collagen film shows good agreement in fibre diameter to hydrated gels imaged under cryogenic conditions, the observed pore area is decreased significantly, indicating the presence of artefactual shrinkage of the collagen network as void spaces normally occupied by water are lost. Under environmental SEM conditions, collagen gel water content cannot be reduced sufficiently to directly visualise collagen fibres of the gel polymer network and ablation damage of the sample appears to be unavoidable, ruling out this method as a recommended approach. Evaporation at $-15°C$ below 100 Pa atmosphere is found to enable collagen fibre visualisation. Low-pressure atmosphere composition is found to further impact the process of gel water evaporation, with a water vapour atmosphere resulting in more gradual loss of water content across the whole surface and introduction of water ice artefacts. In contrast, evaporation under a nitrogen atmosphere reveals a dense 3D polymer network with fine-detail features obscured by a residual hydration shell around hydrophilic collagen fibres.

Control of hydration in the handling of materials in which hydration directly relates to structure and function is critical in producing consistent visualisation for comparative analysis under electron microscopy. Plunge-freezing and cryogenic handling of hydrated collagen gels enables the preservation of micro- and nanoscale structural detail without the use of chemical fixatives to visualise the native state of hydrogel materials. Dehydration of hydrogels can provide accurate information as to molecular organisation of collagen hydrogels such as fibre diameter; however, organisational information such as distribution and density of the collagen fibre network in its hydrated state is lost.

ORCID

Christopher Parmenter https://orcid.org/0000-0002-2092-0555
Paul Roach https://orcid.org/0000-0003-4135-9733

REFERENCES

1. Drury, J. L., & Mooney, D. J. (2003). Hydrogels for tissue engineering: Scaffold design variables and applications. *Biomaterials*, *24*, 4337–4351.
2. Li, J., & Mooney, D. J. (2016). Designing hydrogels for controlled drug delivery. *Nature Reviews Materials*, *1*, 1–17.
3. Moxon, S. R., Cooke, M. E., Cox, S. C., Snow, M., Jeys, L., Jones, S. W., … Grover, L. M. (2017). Suspended manufacture of biological structures. *Advanced Materials*, *29*, 1605594.
4. Hayles, M. F., & De Winter, D. A. M. (2021). An introduction to cryo-FIB-SEM cross-sectioning of frozen, hydrated Life Science samples. *Journal of Microscopy*, *281*, 138–156.
5. Ricard-Blum, S. (2011). The collagen family. *Cold Spring Harbor Perspectives in Biology*, *3*, 1–19.
6. Fu, I., Case, D. A., & Baum, J. (2015). Dynamic water-mediated hydrogen bonding in a collagen model peptide Graphical Abstract HHS Public Access. *Biochemistry*, *54*, 6029–6037.
7. Sebag, J., & Balazs, E. A. (1989). Morphology and ultrastructure of human vitreous fibers. *Investigative ophthalmology & visual science*, *30*(8), 1867–1871.
8. Silver, F. H., Kato, Y. P., Ohno, M., & Wasserman, A. J. (1992). Analysis of mammalian connective tissue: Relationship between hierarchical structures and mechanical properties. *Journal of Long-Term Effects of Medical Implants*, *2*, 165–198.
9. Gillies, A. R., & Lieber, R. L. (2011). Structure and function of the skeletal muscle extracellular matrix. *Muscle & Nerve*, *44*(3), 318–331. https://doi.org/10.1002/mus.22094
10. Guilak, F., Cohen, D. M., Estes, B. T., Gimble, J. M., Liedtke, W., & Chen, C. S. (2009). Control of stem cell fate by physical interactions with the extracellular matrix. *Cell Stem Cell*, *5*, 17–26.

11. Ushiki, T. (2002). Collagen fibers, reticular fibers and elastic fibers. A comprehensive understanding from a morphological viewpoint. *Archives of Histology and Cytology*, *65*, 109–126.

12. Masic, A., Bertinetti, L., Schuetz, R., Chang, S. -. W., Metzger, T. H., Buehler, M. J., & Fratzl, P. (2015). Osmotic pressure induced tensile forces in tendon collagen. *Nature Communications*, *6*, 1–8.

13. Lozano, P. F., Scholze, M., Babian, C., Scheidt, H., Vielmuth, F., Waschke, J., … Hammer, N. (2019). Water-content related alterations in macro and micro scale tendon biomechanics. *Scientific Reports*, *9*(1), 7887.

14. Gul-E-Noor, F., Singh, C., Papaioannou, A., Sinha, N., & Boutis, G. S. (2015). The behavior of water in collagen and hydroxyapatite sites of cortical bone: Fracture, mechanical wear, and load bearing studies. *The Journal of Physical Chemistry. C, Nanomaterials and Interfaces*, *119*, 21528.

15. Fielder, M., & Nair, A. K. (2019). Effects of hydration and mineralization on the deformation mechanisms of collagen fibrils in bone at the nanoscale. *Biomechanics and Modeling in Mechanobiology*, *18*, 57–68.

16. Lees, S. (1986). Water content in type I collagen tissues calculated from the generalized packing model. *International Journal of Biological Macromolecules*, *8*, 66–72.

17. Morin, C., & Hellmich, C., Henits, P. (2013). Fibrillar structure and elasticity of hydrating collagen: A quantitative multiscale approach. *Journal of Theoretical Biology*, *317*, 384–393.

18. Streeter, I., & De Leeuw, N. H. (2011). A molecular dynamics study of the interprotein interactions in collagen fibrils. *Soft Matter*, *7*, 3373–3382.

19. Stylianou, A. (2017). Atomic force microscopy for collagen-based nanobiomaterials. *Journal of Nanomaterials*, *2017*, https://doi.org/10.1155/2017/9234627

20. Andriotis, O. G., Elsayad, K., Smart, D. E., Nalbach, M., Davies, D. E., & Thurner, P. J. (2019). Hydration and nanomechanical changes in collagen fibrils bearing advanced glycation end-products. *Biomedical Optics Express*, *10*, 1841.

21. Uhlig, M. R., & Magerle, R. (2017). Unraveling capillary interaction and viscoelastic response in atomic force microscopy of hydrated collagen fibrils. *Nanoscale*, *9*, 1244–1256.

22. Cen, L., Liu, W., Cui, L., Zhang, W., & Cao, Y. (2008). Collagen tissue engineering: Development of novel biomaterials and applications. *Pediatric Research*, *63*, 492–496.

23. Rajan, N., Habermehl, J., Coté, M. -F., Doillon, C. J., & Mantovani, D. (2007). Preparation of ready-to-use, storable and reconstituted type I collagen from rat tail tendon for tissue engineering applications. *Nature Protocols*, *1*, 2753–2758.

24. Makris, E. A., Responte, D. J., Paschos, N. K., Hu, J. C., & Athanasiou, K. A. (2014). Developing functional musculoskeletal tissues through hypoxia and lysyl oxidase-induced collagen cross-linking. *PNAS*, *111*, E4832–E4841.

25. Grant, C. A., Phillips, M. A., & Thomson, N. H. (2012). Dynamic mechanical analysis of collagen fibrils at the nanoscale. *Journal of the Mechanical Behavior of Biomedical Materials*, *5*, 165–170.

26. Chernoff, E. A. G., & Chernoff, D. A. (1998). Atomic force microscope images of collagen fibers. *Journal of Vacuum Science & Technology A: Vacuum, Surfaces, and Films*, *10*, 596.

27. Bi, X., Li, G., Doty, S. B., & Camacho, N. P. (2005). A novel method for determination of collagen orientation in cartilage by Fourier transform infrared imaging spectroscopy (FT-IRIS). *Osteoarthritis and Cartilage*, *13*, 1050–1058.

28. Lloyd, G. E. (1987). Atomic number and crystallographic contrast images with the SEM: A review of backscattered electron techniques. *Mineralogical Magazine*, *51*, 3–19.

29. Royall, C. P., Thiel, B. L., & Donald, A. M. (2001). Radiation damage of water in environmental scanning electron microscopy. *Journal of Microscopy*, *204*, 185–195.

30. Inoue, N., Takashima, Y., Suga, M., Suzuki, T., Nemoto, Y., & Takai, O. (2018). Observation of wet specimens sensitive to evaporation using scanning electron microscopy. *Microscopy*, *67*, 356–366.

31. Marmorat, C., Arinstein, A., Koifman, N., Talmon, Y., Zussman, E., & Rafailovich, M. (2016). Cryo-imaging of hydrogels supermolecular structure. *Scientific Reports*, *6*, 1–6.

32. Schultz, P. (1988). Cryo-electron microscopy of vitrified specimens. *Quarterly Reviews of Biophysics*, *21*, 129–228.

33. Kaberova, Z., Karpushkin, E., Nevoralová, M., Vetrík, M., Šlouf, M., & Dušková-Smrčková, M. (2020). Microscopic structure of swollen hydrogels by scanning electron and light microscopies: Artifacts and reality. *Polymers (Basel)*, *12*(3), 578.

34. Parmenter, C., Baki, A., & Shakesheff, K. M. (2016). The application of cryogenic focused ion beam scanning electron microscopy to hydrogel characterization. *Microscopy and Microanalysis*, *22*, 192–193.

35. Hurbain, I., & Sachse, M. (2011). The future is cold: Cryopreparation methods for transmission electron microscopy of cells. *Biologie Cellulaire*, *103*, 405–420.

36. Podhorská, B., Vetrík, M., Chylíková-Krumbholcová, E., Kománková, L., Rashedi Banafshehvaragh, N., Šlouf, M., … Janoušková, O. (2020). Revealing the true morphological structure of macroporous soft hydrogels for tissue engineering. *Applied Sciences (Switzerland)*, *10*(19), 6672.

37. Gosden, R. G., Yin, H., Bodine, R. J., & Morris, G. J. (2010). Character, distribution and biological implications of ice crystallization in cryopreserved rabbit ovarian tissue revealed by cryo-scanning electron microscopy. *Human Reproduction*, *25*, 470–478.

38. Danilatos, G. D., & Robinson, V. N. E. (1979). Principles of scanning electron microscopy at high specimen chamber pressures. *Scanning*, *2*, 72–82.

39. Tkaczyk, M., Dragnevski, K., & Edwards, G. (2016). Using the Deben Enhanced Coolstage for in-situ (E)SEM freeze-drying & high resolution imaging of polymer latices. In *European Microscopy Congress 2016: Proceedings*, pp. 267–268. https://doi.org/10.1002/9783527808465.EMC2016.5955

40. Schindelin, J., Arganda-Carreras, I., Frise, E., Kaynig, V., Longair, M., Pietzsch, T., … Cardona, A. (2012). Fiji: An open-source platform for biological-image analysis. *Nature Methods*, *9*, 676–682.

41. Gun'ko, V., Savina, I., & Mikhalovsky, S. (2017). Properties of water bound in hydrogels. *Gels*, *3*(4), 37.

42. Paterson, S. M., Casadio, Y. S., Brown, D. H., Shaw, J. A., Chirila, T. V., & Baker, M. V. (2013). Laser scanning confocal microscopy versus scanning electron microscopy for characterization of polymer morphology: Sample preparation drastically distorts morphologies of poly(2-hydroxyethyl methacrylate)-based hydrogels. *Journal of Applied Polymer Science*, *127*, 4296–4304.

43. Aston, R., Sewell, K., Klein, T., Lawrie, G., & Grøndahl, L. (2016). Evaluation of the impact of freezing preparation techniques on the characterisation of alginate hydrogels by cryo-SEM. *European Polymer Journal*, *82*, 1–15.

44. Koch, M., & Włodarczyk-Biegun, M. K. (2020). Faithful scanning electron microscopic (SEM) visualization of 3D printed alginate-based scaffolds. *Bioprinting*, *20*, e00098.

45. Royall, C. P., & Donald, A. M. (2002). Optimisation of the environmental scanning electron microscope for observation of drying of matt water-based lacquers. *Scanning*, *24*, 305–313.

How to cite this article: Merryweather, D. J., Weston, N., Roe, J., Parmenter, C., Lewis, M. P., & Roach, P. (2023). Exploring the microstructure of hydrated collagen hydrogels under scanning electron microscopy. *Journal of Microscopy*, *290,* 40–52. https://doi.org/10.1111/jmi.13174